Materials Research Proceedings 54 (2025) 150-158 https://doi.org/10.21741/9781644903599-17

Assessing the printability of alginate-cellulose-based inks for syringe extrusion printing

Caterina Pasotti[1,a], Miriam Seiti[1,2,b*], Pieter De Wever[3,c], Paola Ginestra[2,d], Pedro Fardim[3,e], Eleonora Ferraris[1,f]

[1]Department of Mechanical Engineering, Campus De Nayer, KU Leuven, Belgium

[2]Department of Mechanical and Industrial Engineering, University of Brescia, Brescia, Italy

[3]Chemical and Biochemical Reactor Engineering and Safety, Department of Chemical Engineering, KU Leuven, Celestijnenlaan 200f, 3001 Leuven, Belgium

[a]caterina.pasotti@student.kuleuven.be, [b]miriam.seiti@kuleuven.be, [c]pieter.dewever@kuleuven.be, [d]paola.ginestra@unibs.it, [e]pedro.fardim@kuleuven.be, [f]eleonora.ferraris@kuleuven.be

Keywords: Printability Index, Hydrogels, Syringe Extrusion, Process Analysis

Abstract. Syringe extrusion-based printing is a prominent additive manufacturing (AM) technique widely used in biomanufacturing. This technology is cost-effective, scalable, and capable of printing diverse hydrogels and bioinks with viscosities ranging from 30 mPa·s to $6 \cdot 10^7$ Pa·s and resolutions down to 200 μm. The printability of hydrogels typically depends on basic visual assessments, which do not accurately reflect a comprehensive analysis of shape fidelity. This study introduces a quantitative approach with a novel printability index (*Pr*). The *Pr* index comprises four sub-indices: the unit cell factor (circularity), the pattern factor (uniformity of filament width), the unit CAD fidelity, and the filament fidelity (alignment with the CAD model). To validate this index, sodium alginate–cellulose-based hydrogels were formulated and studied by a full factorial design of experiment approach, with *Pr* as response of interest. The inks exhibited a gel-like behavior with shear-thinning characteristics, suitable for (bio)printing. The *Pr* index successfully assessed the printability of such inks, with the cellulose-based ink showing optimal performance (*Pr* = 0.92) at a print speed of 20 mm/s and pressure of 90 kPa. Free-standing structures were further successfully printed, validating the potential of such cellulose-based hydrogels as preferred material. To summarize, this study proposes a *Pr* index which can be widely applied to evaluate the production of structured patterns and adapted for use in various AM technologies. Future studies will be devoted to use the selected hydrogel for bioprinting and 3D cellular differentiation.

Introduction

Syringe extrusion-based printing is a widely recognized additive manufacturing (AM) technology, especially in the biomanufacturing of soft hydrogels applied to tissue engineering (TE) and biomedicine. This technology is cost-effective, scalable, and offers the capability to print a wide range of hydrogels and bioinks, with a viscosity η between 30 mPa·s and $6 \cdot 10^7$ Pa·s, including those of natural, synthetic, and composite origins. Nonetheless, only liquid viscous materials can be processed, and resolutions are limited in the range of (200–2000) μm. Due to the increasing demand for sustainable and biocompatible manufacturing techniques for biomedical and life science applications, the need to ensure good printability, structural stability, and functional performance of biomaterials is crucial, while keeping biocompatibility and precision.

The printability of such hydrogels is defined by the ability to generate a good 3D construct with high shape fidelity and repeatability. Despite the vast adoption of such technique, the use of analytical indices, which address the printability of hydrogels, is uncommon and most assessments only rely on basic visual evaluations, such as comparing the circularity of the unit cell (circular,

irregular, or square) to the chosen pattern, as first reported by Ouyang et al.[1]

In this manuscript, a printability index, *Pr* [#], is proposed as the weighted mean of four sub-indices: i) the unit cell factor, ii) the pattern factor, iii) the unit computer-aided design (CAD) fidelity, and iv) the filament fidelity. All factors have values from 0 to 1, where 1 is ideal and 0 is the worst. To test its validity, *Pr* was here selected as response of interest in a design of experiment (DOE) approach applied for the printing of own-developed alginate-cellulose inks. Alginate is selected being one of the most used bases for hydrogel preparation, especially for 3D printing. Sodium salt alginate (SA) is particularly a natural polysaccharide polymer that is typically obtained from red or brown algae (*Phaeophycean*) or bacteria. Alginate is commonly used in biomedical applications due to its easy processability, fast gelation rate, affordable costs, good biocompatibility, good printability, and tunable mechanical properties.[2] It contains blocks of (1,4)-linked β-D-mannuronate (M) and α-L-guluronate (G) units, which are usually crosslinked with divalent cations (such as calcium chloride, $CaCl_2$).[3] These blocks consist of sequences comprising consecutive M residues (MMMMMM), consecutive G residues (GGGGGG), and alternating M and G residues (GMGMGM).[4]

Alginate is usually selected in combination with other biomaterials in order to enhance the rheological, mechanical and biochemical properties of the resulting bioink. In this work, cellulose is used as co-polymer being a typical solute used with SA in hydrogel formulations as thickener and rheology modifier. Cellulose is an abundant natural biopolymer, constituted by a linear chain of glucose molecules $(C_6H_{10}O_5)_n$ bounded by carbon C1, usually obtained from plant source, such as bamboo, cotton, and algae,[5] or bacteria source (*Pseudomonas* and *Acetobacter*).[6] Cellulose derivates can be produced by chemical or physical modification. Chemically modified cellulose is obtained through degradation and derivatization of hydroxyl groups. Examples include cellulose ethers (such as methyl cellulose and hydroxyethyl cellulose) and cellulose esters (such as cellulose acetate and xanthate). Alternatively, physical modifications can promote surface absorption, mechanical grinding, and swelling, without resulting in a change in the chemical composition. Examples are cellulose nanofibers, cellulose nanocrystals and microcrystalline cellulose, widely used in TE applications. In this study, two cellulose derivates, a carboxymethyl cellulose (CMC) and a cellulose-based product, were chosen.

Rheological properties of these inks were investigated, and their printability was further studied using the *Pr* index in a full-factorial DOE applied on the two main print parameters, that is control pressure and print speed. Among five ink formulations, the best ink was selected and free-standing structures, including a lattice structure and an ear-like scaffold, were successfully 3D printed using the optimized print parameters.

The proposed *Pr* index can be generally exploited to evaluate structured pattern manufacturing and extended to other AM technologies.

Materials and Methods

Material development and characterization. Five ink formulations composed of sodium salt alginate (SA) and two cellulose derivates as rheology modifiers, that is CMC and a cellulose-based product, were own-developed. Each component was slowly added to distilled water (DI), used as main solvent, and then stirred. The SA was mechanically stirred (Heidolph RZR 2041, UK) by adjusting the speed between 800 and 2000 rpm for 40 min, until the SA and other compounds were homogeneously combined, while the cellulose derivates were magnetically stirred (VELP Scientifica Srl, IT). A mortar and pestle were used to eliminate any potential residual of agglomeration. All solutions were stored at 4 °C. Table 1 lists the concentrations for each ink's compound. The rheological properties of each ink were tested using a modular compact rheometer (MCR 702, Anton Paar, CH). Before printing, the inks were loaded in 3 ml syringes equipped with Nordson EFD conical nozzles. Inks were centrifuged at 3200 rpm for 10 min to avoid any presence of bubbles.

Table 1 – Details of the own-developed SA-based ink compositions with cellulose derivates as additives.

Number	Name	Ink composition
0	SA3 (control)	3 w/w% SA
1	SA3-Cel4	3 w/w% SA + 4 w/w% Cel
2	SA3-Cel3	3 w/w% SA + 3 w/w% Cel
3	SA2.5-CMC1.5	2.5 w/w% SA + 1.5 w/w% CMC
4	SA2.5-CMC2.5	2.5 w/w% SA + 2.5 w/w% CMC

The rheological properties of each ink were tested using a modular compact rheometer (MCR 702, Anton Paar, CH). A flow sweep analysis was run to acquire the ink viscosity, shear stress and shear rate, using two parallel rough plates (Ø = 25 mm) which should prevent potential slipping effects. The temperature was set at 20 °C and an oil ring was used to avoid ink evaporation. The storage and loss modulus of the inks were obtained at various angular frequencies ω [rad/s] by a frequency sweep analysis. A small-amplitude oscillatory shear (SAOS) technique and two parallel plates were used to have a general overview of the hydrogels' linear-viscoelastic regime (LVE).

The flow characteristics of the inks were determined according to the Power-Law Equation (Eq. 1):

$$\eta = K * (\dot{\gamma})^{n-1}, \quad (1)$$

in which η is the dynamic viscosity [Pa·s], $\dot{\gamma}$ is the shear rate [1/s], K and n are the shear-thinning coefficients. Specifically, K [Pa·s^n] is the fluid consistency index, and n is the flow behaviour index.[7]

Process investigation and methodology. A pneumatic micro-extrusion Inkredible$^+$ 3D bioprinter by Cellink (Bico Company, SE) was used to perform the experiments in ambient conditions (22 °C, 55 %rh). An external oil-free air compressor device provides the pneumatic pressure, which is controlled by a knob. The printer offers a layer resolution of 100 µm with a positioning precision of 10 µm on the x and y axes, and of 2.5 µm on the z-axis. The hydrogel's viscosity range is from 0,001 to 250 Pa·s, while the control pressure is between 5 and 400 kPa, with a sensitivity of 0.8 kPa. The dual print head and the print bed can be heated up from room temperature (RT) up to 130 °C and 65 °C, respectively. Printer calibration was executed in accordance with the manufacturer's instructions. A conical nozzle with smooth flow tapered tip (25 G) was selected. Print patterns were designed with the software Idea Maker, then the *.stl* files were sliced and converted to Gcodes. The Gcodes were manually modified with the Repetier Host software to add specific Cellink Gcodes commands.

A full-factorial DOE of the type 3^k ($k > 0$), with $k = 2$ (three repetitions), was then carried out to examine the effect of print parameters printing speed, s (10; 20; 30) mm/s, and control pressure, p [kPa] (ink dependent). A mesh 20 x 20 mm with an infill at 40% was printed for each data point. All printed meshes were then crosslinked with $CaCl_2$ at 4 w/v% for 5 min. For the print tests, glass slides (Superfrost, VWR, BE) and petri dishes were employed as substrate. Before usage, the glass slides were ultrasonically cleaned with DI and isopropanol (IPA) (Sigma Aldrich, BE) at T = 25 °C for 15 min. Table 2 reports details of the experimental tests performed.

Table 2 – Details of the experimental tests performed on own-developed SA-cellulose inks.

Full factorial design 3^k (k = 2) for printed meshes			
Factors	Levels		
Pressure, *p* [kPa]	Ink dependent (see Table 3)		
Print Speed, *s* [mm/s]	4	8	12
Repetitions [#]	3		
General response	Printability Index, *Pr* [µm]		
Sub-indices	Q1 [#], Q2 [#], Q3 [#], Q4 [#]		
Fixed Parameters	Values		
Sample design	Mesh (20x20 mm)		
Substrate	Glass slides, VWR Superfrost® Plus Micro Slide		
Nozzle diameter, *Ø* [G]	25		
Stand-off distance, *z* [mm]	0.1		
Number of layers, *n* [#]	1		

Printed samples characterization. A *Pr* [#] index was evaluated considering the arithmetic mean (am) of four sub-indices: i) the unit cell factor (Q1), ii) the pattern factor (Q2), iii) the unit CAD fidelity (Q3), and iv) the filament fidelity (Q4). The uniformity factors (Q1 and Q2) evaluate the homogeneity of the mesh, while the shape fidelity factors (Q3 and Q4) the deviation from the theoretical CAD design. In details, Q1 calculates how the unit cell is like a square. The circularity (*C*) of the pores and Q1 were calculated according to the formulas given by Ouyang et al.[8] (Eq. 2):

$$Q1 = \frac{\pi}{4}\frac{1}{C} = \frac{L^2}{16A} \quad , with\ C = \frac{4\pi A}{L^2} \tag{2}$$

where *L* [mm] is the perimeter and *A* [mm^2] the area of the pores, respectively. This means that, in an ideal condition of hydrogel gelation and printability, each pore of the printed mesh is equal to the CAD design (a square of 1 x 1 mm), thus $C = \frac{\pi}{4}$ and $Q1 = 1$. In over-gelation or under-gelation conditions, the index will be $Q1 > 1$ (irregular shape) or $Q1 < 1$ (like a circular shape) respectively. In case $Q1 > 1$, the value is not acceptable and considered. For each mesh, the unit cell Q1 was measured 15 times from at least 2 samples per printing condition. Q2 assesses the uniformity of filament width in both the x and y axes; it was quantified by measuring a total of 4 cross-like intersections for each printing condition and calculating their standard deviation, which in the ideal case of optimal repeatability is equal to 0. Q3 evaluates the resemblance of the printed unit cell to the CAD design (Eq. 3), while Q4 measures how closely the printed filament matches the CAD strand, which corresponds to the nozzle diameter (Eq. 4). The unit cell CAD area was equal to 1 mm^2 and the CAD strand was 0.25 mm wide.

$$Q3 = 1 - \left[\frac{(CAD\ cell\ unit\ area - Printed\ cell\ unit\ area)}{CAD\ cell\ unit\ area}\right] \tag{3}$$

$$Q4 = 1 - \left[\frac{(CAD\ filament\ witdh - Printed\ filament\ witdh)}{CAD\ filament\ witdh}\right] \tag{4}$$

For all factors, the ideal condition is a value equal to 1. The *Pr* index was obtained as (Eq. 5):

$$Pr = am\left(w_{Q1} \cdot Q1, w_{Q2} \cdot Q2,\ w_{Q3} \cdot\ Q3, w_{Q4} \cdot Q4\right),\ 0 \le Pr \le 1 \tag{5}$$

With (Eq. 6):

$$\sum w_{Q1}, w_{Q2},\ w_{Q3}, w_{Q4} = 1. \tag{6}$$

The weights were selected in such a way that the parameters which had the most impact on the printability were Q1 and Q2 ($w_{Q1} = w_{Q2} = 0.3$), while $w_{Q3} = w_{Q4} = 0.2$. In fact, among all indexes, a mesh with a square unit cell and uniform filaments were considered as the most crucial factors in obtaining a high printability.

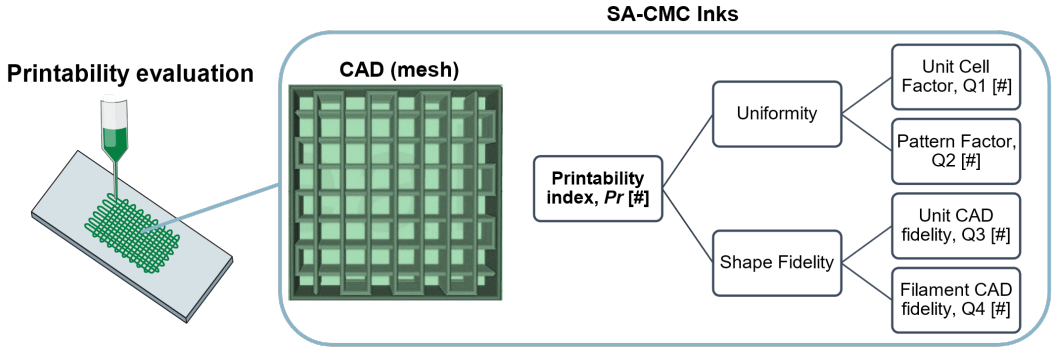

Figure 1 – Graphical representation of the Pr index evaluation applied on 3D printed SA-cellulose inks.

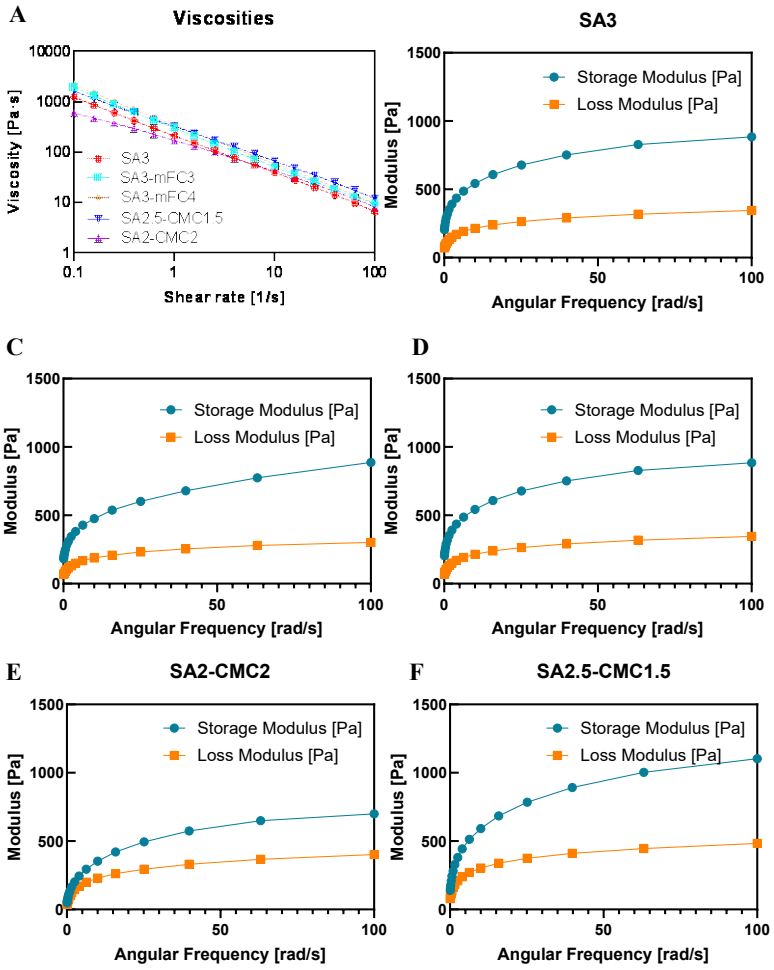

Figure 2 – Rheological properties of SA-cellulose inks: a) Viscosity of all inks; storage and loss modulus as function of the frequency for b) SA3, c) SA3-Cel3, d) SA3-Cel4, e) SA2-CMC2, and f) SA2.5-CMC1.5.

Fig. 1 illustrates how the *Pr* index calculation. Finally, a filament collapse test was conducted to assess any material collapse. A platform was created using a 3D printer Prusa (CZ) and designed with Idea Maker software. This platform consisted of six pillars spaced at intervals of 1, 2, 3, 4, and 6 mm. The dimensions of the pillars were 10 x 2 x 7 mm, and the lower platform measured 10 x 50 x 3 mm. For each ink, a single filament line was printed on the top of this platform.

Results and Discussion

Fig. 2 outlines the viscosity of SA-cellulose inks as a function of the shear stress, showing a shear thinning behaviour. SA3 has a decrease in viscosity from 1238 Pa·s at 0,1 s^{-1} to 7 Pa·s at 100 s^{-1}, SA3-Cel3 from 1923 Pa·s at 0,1 s^{-1} to 9 Pa·s at 100 s^{-1}, SA3- Cel4 from 2165 Pa·s at 0,1 s^{-1} to 10 Pa·s at 100 s^{-1}, SA2-CMC2 from 602 Pa·s at 0,1 s^{-1} to 8 Pa·s at 100 s^{-1}, and finally SA2.5-CMC1.5 from 1604 Pa·s at 0,1 s^{-1} to 12 Pa·s at 100 s^{-1}. All inks well fit the range for syringe-extrusion printability, calculated using the Power Law Equation, [7] that is SA3 (K = 214.8, n = 0.25), SA3-Cel3 (K = 306.2, n = 0.23), SA3-Cel4 (K = 346.7, n = 0.22), SA2-CMC2 (K = 163.7, n = 0.94), and SA2.5-CMC1.5 (K = 322.8, n = 0.93). The storage and loss moduli of SA-cellulose inks are reported in Figs. 2b-f, demonstrating in every condition storage moduli higher than loss moduli, thus resembling a gel-like behaviour.

Table 3 – Geometrical analysis of printed meshes (3 repetitions each) in terms of Q [#] factors and the final Pr [#], based on the different DOE conditions for the SA-based inks with cellulose additives.

Full factorial analysis 2^k (k > 0), k = 3 on printed meshes, (μ ± σ)					
Condition (s [mm/s], p [KPa]	**Q1 [#]**	**Q2 [#]**	**Q3 [#]**	**Q4 [#]**	**Pr [#]**
Ink SA3-Cel3					
S0P0 (10-90)	0.91	0.99	0.91	0.99	0.95
S0P1 (10-100)	0.88	0.99	0.88	0.98	0.94
S0P2 (10-110)	0.88	1.00	0.93	0.99	0.95
S1P0 (20-90)	0.92	0.99	0.96	0.99	0.97
S1P1 (20-100)	0.88	1.00	0.95	0.99	0.95
S1P2 (20-110)	0.87	1.00	0.96	0.99	0.95
S2P0 (30-90)	0.87	1.00	0.97	0.99	0.95
S2P1 (30-100)	0.92	1.00	0.96	0.99	0.96
S2P2 (30-110)	0.92	0.97	0.98	0.99	0.96
Ink SA3-Cel4					
S0P0 (10-70)	0.94	1.00	0.94	0.99	0.97
S0P1 (10-80)	0.89	0.99	0.92	0.79	0.91
S0P2 (10-90)	0.84	1.00	0.89	0.83	0.89
S1P0 (20-70)	0.92	0.99	0.95	0.94	0.97
S1P1 (20-80)	0.89	0.99	0.93	1.00	0.86
S1P2 (20-90)	0.87	0.99	0.91	0.72	0.89
S2P0 (30-70)	0.93	1.00	0.96	1.00	0.97
S2P1 (30-80)	0.90	1.00	0.94	0.99	0.96
S2P2 (30-90)	0.94	0.99	0.92	0.99	0.96
Ink SA2.5-CMC1.5					
S0P0 (10-75)	0.87	1.00	0.97	0.99	0.95
S0P1 (10-90)	0.85	1.00	0.92	0.99	0.93
S1P0 (20-75)	0.89	0.98	0.96	0.98	0.95
S1P1 (20-90)	0.84	0.98	0.95	0.99	0.93
S2P0 (30-75)	0.86	0.99	0.96	0.99	0.94
S2P1 (30-90)	0.83	0.97	0.94	0.99	0.92
Ink SA2-CMC2					
S0P0 (10-70)	0.82	0.99	0.92	0.99	0.92
S1P0 (20-70)	0.83	0.99	0.92	0.83	0.90
S2P0 (30-70)	0.81	0.96	0.95	0.81	0.88

All inks were studied according to a full factorial design for the printing of a mesh structure. The CMC-based inks are highly affected by the control pressure, resulting in a narrower pressure range for successful printing. Conversely, the Cel product extends the printability range, enabling satisfactory printing within a wider pressure range. Table 3 lists the values for each Q index and the final *Pr* of printed meshes (3 repetitions each) obtained from the different DOE conditions for each ink developed. The *Pr* values are also visually reported in Fig. 3.

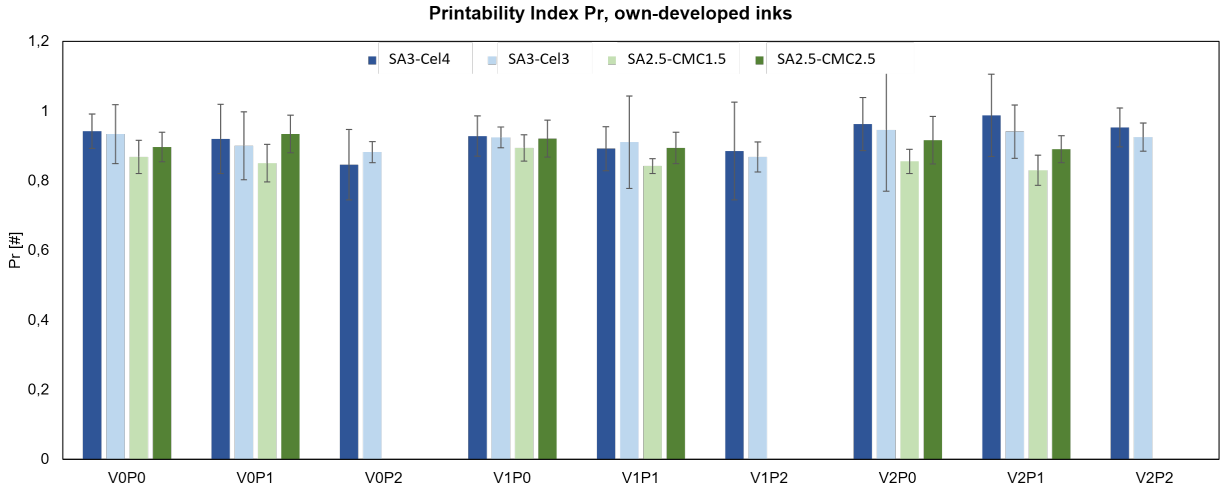

Figure 3 – Printability indexes, Pr, for SA-cellulose inks in the analysed printing conditions.

SA3-Cel3 is chosen as the best overall ink since it displays an excellent printability under all pressure and print speed combinations examined, with the best condition being S1P0 (20 mm/s, 90 kPa). The Q4 value is significantly high (0.99), primarily due to the extruded filament width being narrow and closely resembling the size of the nozzle diameter. As a general trend, it is evident that an increase in pressure results in a decrease in all Q values. This is because a higher pressure implies a greater applied force on ink extrusion, which in turn leads to an increase in the material deposition. Regarding the SA3-Cel4 ink, the best condition is obtained at P0 (70 kPa). Contrarly, only few conditions are printable in the form of meshes and subjected to analysis for both the inks containing CMC. The unit cell with these inks indeed visually resembles a circle more than a square, which is reflected in lower Q1 values. Similarly to the previous inks, the best conditions for the SA2.5-CMC1.5 formulation are found at the lowest values of pressure and speed, that is S0P0 (10;75), while for the SA2-CMC2 ink, only a limited number of conditions give satisfactory results, with just P0 being acceptable. In this instance, the Q1 value is closer to 0.785 (perfect circle) rather than 1, and the line width, although homogenous across the entire mesh, exceeds the nozzle diameter, as indicated by the Q4 value.

Fig. 4 presents representative images of the printed meshes and their filament collapse test of all types of inks. Particularly, for the SA3-Cel3 the mesh is uniform, despite some defects are visible due to the potential presence of air bubbles in the syringe. Moreover, rounded pores rather than squared are clearly visible for the SA2-CMC2 ink. Filament collapse tests were performed to verify the capability of the inks to sustain 3D printed constructs before and after crosslinking in bath. SA3-Cel3 and SA3-Cel4 show a good filament deposition and SA2-CMC2 and SA2.5-CMC1.5 do not show any collapse, although their filament is extremely thin due to their low viscosity. This indicates that due to a higher diffusion coefficient, when two filaments are deposited, they tend to merge into a single filament, which is not an ideal characteristic for 3D printed structures. Lastly, Fig. 5 illustrates two 3D printed cubes (measuring 15 x 15 x 3 mm and 20 x 20 x 5 mm) and a self-supporting human ear-like structure produced with the SA3-Cel3 ink.

Specifically, these cubes exhibit a strong layer support, but there is a noticeable material collapsing at the centre of the cube.

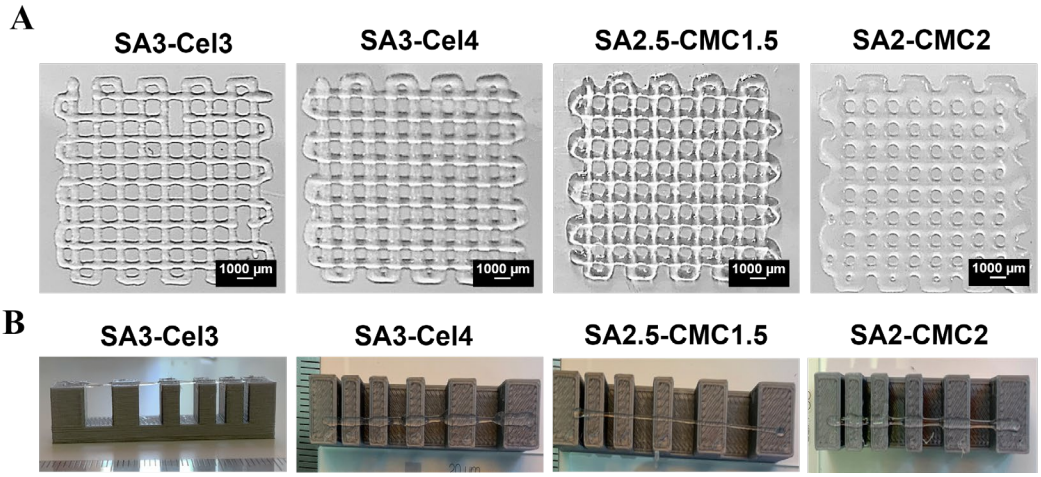

Figure 4 – Representative images of SA-cellulose inks related to A) printed meshes and B) filament collapse tests.

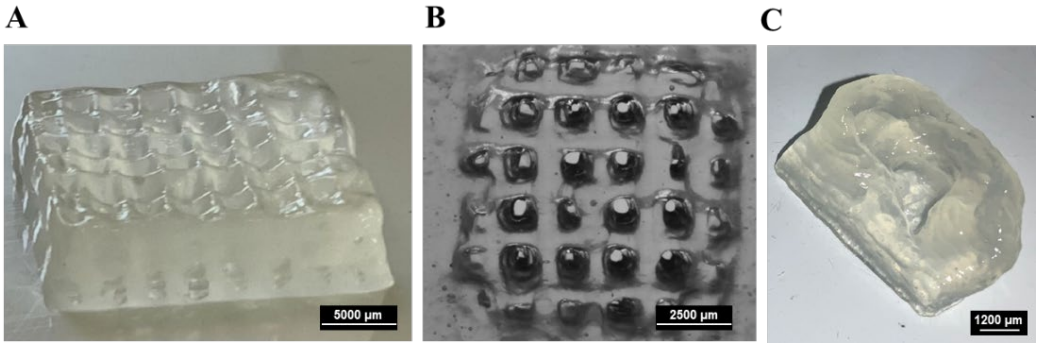

Figure 5 – Optical images of two 3D SA3-Cel3 printed cubes at the dimensions a) 15x15x3 mm and b) 20x 20x5 mm), and c) a self-supporting human ear-like structure.

Conclusion and Future Perspectives

This manuscript reports the quantitative assessment of printability applied to hydrogels using the syringe extrusion-based technology. A printability index, *Pr* [#], was calculated as the sum of four sub-indices: i) the unit cell factor (circularity), ii) the pattern factor (the uniformity of filament width along x and y axes) iii) the unit CAD fidelity, and iv) the filament fidelity (how closely the printed filament matches the CAD strand). To validate the *Pr* index proposed, free-standing SA-cellulose based hydrogels were formulated and their rheological behaviour was studied. All inks showed a gel-like behaviour and rheological properties in line with (bio)-printing requirements.

Key findings are:

- All inks were successfully printable, showing a good shear thinning behavior: viscosities 1200- 2200 Pa·s at 0.1 s^{-1}, 7-12 Pa·s at 100 s^{-1}; storage modulus > loss modulus (gel-like);
- *Pr* index was effectively validated for all inks;
- Best ink: cellulose-based product is preferred over CMC as rheology modifier. Excellent *Pr* = 0.92, optimal at *s* = 20 mm/s, *p* = 90 kPa.

Future research will focus on the printing of the best ink with embedded mesenchymal stem cells for skin tissue bioprinting and 3D cellular differentiation.

References

[1] L. Ouyang, R. Yao, Y. Zhao, W. Sun, “Effect of bioink properties on printability and cell viability for 3D bioplotting of embryonic stem cells”, Biofabrication 2016, 16;8(3):035020. https://doi.org/10.1088/1758-5090/8/3/035020

[2] P. P. Shah, H. B. Shah, K. K. Maniar, and T. Özel, “Extrusion-based 3D bioprinting of alginate-based tissue constructs,” Procedia CIRP 2020, 95:143–148. https://doi.org/10.1016/J.PROCIR.2020.06.007.

[3] K. Y. Lee and D. J. Mooney, “Alginate: Properties and biomedical applications,” Prog. Polym. Sci., 2012, 37(1):106–126. https://doi.org/10.1016/J.PROGPOLYMSCI.2011.06.003

[4] N. M. Sanchez-Ballester, B. Bataille, and I. Soulairol, “Sodium alginate and alginic acid as pharmaceutical excipients for tablet formulation: Structure-function relationship,” Carbohydr. Polym. 2021, 270:118399. https://doi.org/10.1016/J.CARBPOL.2021.118399.

[5] P. BÃcguin and J.-P. Aubert, “The biological degradation of cellulose,” FEMS Microbiol. Rev. 1994, 13(1):25–58. https://doi.org/10.1111/J.1574-6976.1994.TB00033.X

[6] R. J. Hickey and A. E. Pelling, “Cellulose biomaterials for tissue engineering,” Front. Bioeng. Biotechnol. 2019, 7:45. https://doi.org/10.3389/FBIOE.2019.00045/BIBTEX

[7] E. Reina-Romo, S. Mandal, P. Amorim, V. Bloemen, E. Ferraris, and L. Geris, “Towards the Experimentally-Informed In Silico Nozzle Design Optimization for Extrusion-Based Bioprinting of Shear-Thinning Hydrogels,” Front. Bioeng. Biotechnol., 2021, (9):701778. https://doi.org/10.3389/FBIOE.2021.701778/BIBTEX

[8] “Effect of bioink properties on printability and cell viability for 3D bioplotting of embryonic stem cells,” 2016, 8(3):035020 doi: 10.1088/1758-5090/8/3/035020